

# Radio-Quiet Quasars in the Direction of the Northern Hubble Deep Field

Chris Impey and Cathy Petry

*Steward Observatory, The University of Arizona, Tucson, AZ 85721*

## ABSTRACT

We match quasars discovered in a multi-color survey centered on the northern Hubble Deep Field (HDF) with radio sources from an ultra-deep radio survey. Although 3 out of 12 quasars are detected at a level below 0.2 mJy at 1.4 GHz, all of the quasars in the search area are radio-quiet by the criterion  $L_r < 10^{25} h_{50}^{-1} \text{ W Hz}^{-1}$ . We combine this information with other radio surveys of quasars so as to break the degeneracy between redshift and luminosity. In the redshift range  $0.02 < z < 3.64$ , the radio-loud fraction increases with increasing optical luminosity, consistent with some degree of correlation between the non-thermal optical and radio emissions. More tentatively, for low luminosity quasars in the range  $-22.5 < M_B < -25$ , the radio-loud fraction decreases with increasing redshift. We can infer from this that the radio luminosity function evolves more slowly than the optical luminosity function. The mechanism that leads to strong radio emission in only a small fraction of quasars at any epoch is still unknown.

*Subject headings:* quasars: general—radio continuum: general—surveys

## 1. Introduction

Nearly forty years after their discovery, it is still not clear what determines the degree of radio emission from quasars. Although quasars were first discovered at radio wavelengths (Schmidt 1963), it has long been known that most quasars emit a very small fraction of their total power in the radio (Sandage 1965). When radio observations had limited sensitivity, it made sense to talk about two populations: radio-loud and radio-quiet. However, Kellermann et al. (1989, 1994) detected about 90% of objects in the mostly low redshift Palomar-Green Bright Quasar Survey (BQS). This survey revealed that (a) the radio luminosity range of the BQS is almost disjoint with that of radio-selected quasars, (b) the ratio of radio to optical power is continuous and spans at least five orders of magnitude, and (c) while most quasars are radio-quiet, few if any are truly radio-silent.

In the absence of a physical understanding of the radio emission in most quasars, it is not clear how best to define radio-loudness. Many workers have used the ratio of radio-to-optical power,

$R$ , to characterize the degree of radio emission (Kellermann et al. 1989; Hooper et al. 1996; Bischof and Becker 1997). This has an advantage as a distant-independent quantity, but its interpretation is only physically meaningful if radio and optical luminosity are correlated. Peacock et al. (1986) and Stocke et al. (1992) showed that this is unlikely to be the case. Another common definition of radio-loud is based on a radio luminosity boundary,  $L_r > 10^{25} h_{50}^{-1} \text{ W Hz}^{-1}$  (Hooper et al. 1996; Bischof and Becker 1997). Radio luminosity can be interpreted in terms of a physical model. The choice of  $\log L_r = 25$  for radio-loud is convenient since it corresponds to a typical  $\sim 1$  mJy detection limit for a quasar with  $M_B = -26$  at  $z \sim 1$ . Radio-loudness is an arbitrary concept in the sense that no one has convincingly demonstrated that the distributions of either radio luminosity or radio-to-optical power are bimodal.

Demographic studies of the radio emission from quasars are affected by the fact that the upper bounds in a detection experiment are correlated with redshift. Different samples must therefore be combined to break the degeneracy between luminosity and redshift. The only way to study low luminosity quasars at high redshift is to combine a faint optical survey with extremely sensitive radio observations. We have chosen to do this in the direction of the northern Hubble Deep Field (HDF), a small region of sky which is at the locus of a wide range of extragalactic studies (Williams et al. 1996). In §2 of this paper, we use a recently published deep radio survey to measure the radio luminosities of quasars found in a one square degree region centered on the HDF. In §3, we combine this sample with other quasar surveys to study the radio-loud fraction as a function of redshift and luminosity. We present conclusions in §4. Modelling of quasar evolution and speculation as to the nature of the radio emission mechanism is deferred to a future paper. We use  $H_0 = 50 \text{ kms}^{-1} \text{ Mpc}^{-1}$  and  $q_0 = 0.5$  ( $\Lambda = 0$ ) throughout for the calculation of luminosity.

## 2. Identifying Optically Faint Quasars with Weak Radio Sources

The northern Hubble Deep Field, along with its southern twin, has motivated a broad array of projects designed to measure the luminous content of the universe out to high redshift. We have been carrying out multi-color surveys of optically faint quasars in one square degree regions centered on each of the deep fields. The quasars will be used to thread these volumes with absorption sightlines, and to compare the location of the absorbers with the large scale structures measured by pencil beam redshift surveys of galaxies (Cohen et al. 1996; Steidel et al. 1996; Hogg et al. 1998). Our first paper reported 30 quasars in the magnitude range  $17.6 < B < 21.0$  and the redshift range  $0.44 < z < 2.98$  (Liu et al. 1999). An independent group is working on quasar selection in a smaller region centered on the HDF (Vanden Berk et al. 2000), and they find an additional 4 quasars with  $B \lesssim 21$ .

To complement the optical imaging with the Hubble Space Telescope (HST), Richards et al. (1998) have carried out a deep radio survey of the HDF down to a  $5\sigma$  limit of  $9 \mu\text{Jy}$  at 8.5 GHz. More recently, Richards (1999) presented a catalog of 372 radio sources (1.4 GHz) within 20 arcmin

of the HDF, with a  $3\sigma$  sensitivity limit ranging from  $40 \mu\text{Jy}$  at the center of the field to  $230 \mu\text{Jy}$  at a radius of 20 arcmin. The strongest sources in the sky are radio galaxies and quasars in roughly equal numbers. At flux levels a million times lower, the radio source population is likely to be composed primarily of star-forming disk galaxies, with a relatively small component of quasars and other AGN (Richards et al. 1998). The advantage of such a sensitive radio survey for our purposes is the fact that quasars at redshifts of  $1 < z < 2$  can be detected down to the traditional boundary between radio-loud and radio-quiet quasars.

Figure 1 shows the distribution of HDF radio sources from Richards (1999), plotted as open circles, along with the distribution of spectroscopically confirmed quasars, plotted as stars. There are 34 quasars within a one square degree area centered on the HDF, 30 of which come from Liu et al. (1999) and 4 of which are added from Vanden Berk et al. (2000). Since both studies used a UVX selection technique and found almost all their quasars in the magnitude interval  $19 < B < 21$ , it is appropriate to combine them.

In a detection experiment such as this, we must bear in mind the fact that the HDF is not a truly random patch of sky in terms of numbers of strong radio sources (Williams et al. 1996). To allow very deep radio observations, the field was chosen such that there was no source stronger than 1 mJy in the primary beam of the VLA at 8.5 GHz. The full sample of Richards et al. (1998) has 29 sources within 4.6 arcmin of the HDF center. However, our experiment is carried out over the substantially larger field of the 1.4 GHz observations (Richards 1999). For the observed median spectral index of 0.63 (Richards 1999), 1 mJy at 8.5 GHz corresponds to 3.1 mJy at 1.4 GHz. There are 9 sources stronger than 3.1 mJy over the 1.4 GHz field of view, or a surface density of 0.0072 sources per square arcminute. The expected number of sources in the smaller region of the 8.5 GHz data is therefore only 0.48. Thus the pre-ordained absence of a source in the central region is not a large perturbation on the statistics of our experiment. In addition, the central region is only 5.3% of the total area of our identification experiment.

A potentially more serious issue is incompleteness in the quasar surveys. The radio survey is uniform down to a particular flux limit, but multicolor quasar selection is not perfectly efficient, and not all candidates brighter than  $B = 21$  have had confirming spectroscopy. This means that the region could contain radio sources identified with unrecognized quasars, which would bias the identification process to lower radio-to-optical flux ratios. In practice, we believe this is not an important effect. The UVX technique is known to be efficient out to  $z \sim 2.5$ , which encompasses the quasars used in this study (Hewett and Foltz 1994). The observed surface density of  $34 \text{ deg}^{-2}$  is in excellent agreement with the highest surface densities ever measured down to this magnitude level (Zitelli et al. 1992; Hall et al. 1996).

There are 12 quasars in the region sampled by the deep VLA observations, as outlined by the circle in Figure 1. These quasars can be identified by positional coincidence with the radio sources. The rms astrometric errors on the radio and optical positions are  $0.03''$  and  $0.5''$ , respectively (Richards 1999; Vanden Berk et al. 2000). With accurate positions and a low surface

density of quasars and radio sources, there is a small probability of a chance coincidence within three times the rms positional error. However, Figure 1 shows that the HDF sources are centrally concentrated, due to attenuation by the primary beam pattern. A statistical test confirms that the radial distribution of radio sources departs from the expectation for a random distribution at more than the 99.9% confidence level. By contrast, the quasar distribution within one square degree is consistent with a random distribution. This means that the probability of a chance coincidence is higher towards the center of the HDF, and it indicates that we should carry out a more rigorous procedure before declaring a radio counterpart.

The results of the identification procedure are summarized in Table 1. For each of the 12 confirmed quasars within the circular region measured by the VLA, we select the nearest radio source as a potential counterpart. The first five columns of Table 1 give the name, J2000 position,  $B$  magnitude and redshift of the 12 quasars. The simulation procedure takes into account the different surface densities of quasars and radio sources and the fact that the radio source distribution shows a radial gradient. We randomly reposition the 34 quasars within the one square degree and repeat this 1500 times. The radial distance to the field center,  $r$ , and the angular distance to the nearest neighbor radio source,  $\theta_{\text{nn}}$ , are saved for each of these 51,000 random quasar placements. Then, for each of the 12 quasars, we form the distribution of  $\theta_{\text{nn}}$  for random quasars falling in an annulus 100 arcseconds wide centered on the radial distance of each quasar from the center of the HDF.

The nearest neighbor distributions for this random experiment are shown in Figure 2. Each panel in the figure is labelled with four items. The first is the quasar name. The second is the radial distance of that quasar from the center of the HDF. The histograms show how the mean nearest neighbor distance depends on  $r$  — the surface density of radio sources is highest near the HDF, so the nearest neighbor distances will on average be smallest. The overall number of trials was chosen so that there were at least 1000 measurements in each histogram. The third item labelled is the actual offset of that quasar from the nearest radio source,  $\theta_{\text{nn}}$  (column 8 in Table 1), marked by a vertical dotted line in the figure. The fourth item is the fraction of trials in the random placement experiment where the quasar had an angular distance of  $\theta_{\text{nn}}$  or smaller from the nearest radio source. Equivalently, it is the probability,  $p$ , that the actual nearest neighbor is a chance counterpart. This number can easily be converted into a percentage confidence limit on the identification,  $(1 - p)/100$ .

Three out of 12 of the quasars have weak radio sources within 1.5 arcseconds, or within three times the sum of the radio and optical position errors added in quadrature. These quasars are therefore identified with greater than 99.5% confidence. It is clear that the identification procedure is robust, since none of the other nine quasars have radio sources within 15 arcseconds. The probability  $p$  is strongly bimodal; three quasars have  $p < 0.002$  (taking into account the statistical accuracy due to the number of points generated for each Monte Carlo histogram), and the other nine have  $p > 0.18$ . To ensure uniqueness, we inspected the 2nd and 3rd nearest neighbors for the three quasars with close companions. The nearest neighbor is by far the most likely true

counterpart with  $p > 0.23$  in all cases, except for the 2nd nearest neighbor to J123800+6213 which has  $p = 0.02$ . Radio fluxes for the three new identifications are listed in the last column of Table 1. The other nine quasars are assigned a  $3\sigma$  upper bound based on the quoted formal completeness limit of  $40 \mu\text{Jy}$  with a scaling by the instrumental gain as presented in Figure 3 of Richards (1999).

Richards et al. (1998) found no quasar or AGN identifications with sources from their 8.5 GHz survey. We can use our results to put an approximate upper bound on the quasar component of the 1.4 GHz survey. Only 3 out of 372, or about 1%, faint radio sources are identified with quasars. We can scale this number up by a factor of 6 to account for 50% incompleteness due to color selection, and at most a factor of 3 increase in optical quasar counts down to  $B \sim 24$  (Boyle et al. 1988). Thus, we predict no more than  $\sim 5\%$  of ultrafaint radio sources can be quasars of *any* optical brightness. This conclusion is firm because the optical survey is deep enough to have seen all the way through the quasar luminosity function for all reasonable cosmologies, and our existing identifications and limits are near the lower bound of the distribution of radio-to-optical flux ratios.

### 3. Radio-Loud Fraction as a Function of Redshift and Luminosity

As stated in the introduction, we prefer to characterize quasars by their radio luminosity rather than their radio-to-optical luminosity ratio, since emissions in the two wavelength regimes appear to not be closely related. Early workers suspected that there were distinct radio-loud and radio-quiet categories of quasars (Kellermann et al. 1989; Miller et al. 1990; Stocke et al. 1992; Visnovsky et al. 1992). However, the onset of the radio-quiet population happens to correspond to the typical flux limit of a VLA snapshot, so the evidence for bimodality was never compelling. As sample sizes have increased, the evidence for two populations has weakened (Hooper et al. 1996; Goldschmidt et al. 1999; Bischof and Becker 1997). Kellermann et al. (1989) established the procedure that has become standard for most papers in this field, defining a monochromatic radio luminosity in the rest frame and assuming that the radio emission is isotropic, with units of  $\text{W Hz}^{-1}$ . Radio luminosity is a continuous variable in the quasar population, but  $L_r > 10^{25} h_{50}^{-1} \text{W Hz}^{-1}$  is a useful definition of radio-loudness, because it corresponds to the beginning of the tail of the distribution. It is also roughly equivalent to the definition of Goldschmidt et al. (1999),  $L_r > 10^{24} h_{50}^{-1} \text{W Hz}^{-1} \text{sr}^{-1}$ .

In this section, we combine the HDF quasar sample with other samples to explore the dependence of the radio-loud fraction on redshift and luminosity. The calculation of all distance-dependent quantities assumes  $H_0 = 50 \text{ km s}^{-1} \text{ Mpc}^{-1}$  and  $q_0 = 0.5$  ( $\Lambda = 0$ ). Rest frame radio luminosities are calculated for an observed flux at 5 GHz. This matches the frequency of BQS data; radio k-corrections for other samples assume a radio spectral index  $\alpha = -0.5$  ( $S_\nu \propto \nu^\alpha$ ). Rest frame absolute magnitudes for the BQS are adopted from Kellermann et al. (1989). The calculation of rest frame absolute magnitude for all other samples uses the k-corrections calculated by Hooper et al. (1995) using a composite LBQS spectrum. The typical uncertainty in these derived

quantities for a particular quasar are  $\sim 0.6$  mag for  $M_B$  (Hooper et al. 1995) and  $\sim 0.15$  for  $\log L_r$  (Aller et al. 1992). The large uncertainty in optical luminosity is due to source variability and the large dispersion in rest frame UV to optical spectral indices. We note that these uncertainties are small compared with the overall range of radio ( $\times 10^5$ ) and optical ( $\times 10^3$ ) luminosity.

Figure 3 shows the coverage of the various samples in terms of linear look-back time and optical luminosity. Equivalent values of redshift are also plotted. The diamonds show the 114 quasars of the optically bright BQS (Kellermann et al. 1989, 1994). The open circles show the 367 quasars with radio measurements from the LBQS (Visnovsky et al. 1992; Hooper et al. 1995, 1996). We choose not to augment this with additional matches in large area surveys like FIRST (White et al. 1997) and NVSS (Condon et al. 1998), because those surveys have 2-6 times lower sensitivity limits. The stars show 87 quasars from the Edinburgh survey (Goldschmidt et al. 1999), which covers a similar region of the redshift-luminosity plane to the LBQS. The twelve new HDF quasars are shown as filled circles in Figure 3. The dotted lines show the plane divided up into equal sized regions of look-back time and absolute magnitude. The highest redshift slice encompasses the epoch of maximum quasar space density. The lower redshift slices span the time over which the space density has declined by two orders of magnitude to the present epoch. The radio-loud fractions in these intervals of look-back time and optical luminosity are investigated in the subsequent analysis.

The intercomparison of samples with bright and faint optical limits allows us to break the degeneracy between redshift and luminosity which exists for any single, flux-limited sample. With a bright magnitude limit and wide area sky coverage, the BQS includes some of the most optically luminous quasars known. However, evidence that the BQS is incomplete (Goldschmidt et al. 1992; Grazian et al. 2000), along with the possibility that the incompleteness depends on radio properties (Peacock et al. 1986; Miller et al. 1993; Hooper et al. 1996), leads us to be cautious in drawing conclusions that depend only on the BQS. The LBQS is a homogeneous survey with a well understood selection function (Hewett et al. 1995). Compared to the BQS, the LBQS reaches lower optical luminosities at a given redshift and higher redshifts at a given optical luminosity. Even though the HDF sample is small, Figure 3 shows that it covers an important range of parameter space at low optical luminosity and moderate redshift.

Figure 4 shows absolute magnitude plotted against radio luminosity for the three samples that cover approximately the same redshift range: the HDF, LBQS and Edinburgh samples. Symbols are the same as in Figure 3. Upper limits are plotted as arrows for the HDF quasars; a box outlines the region containing the upper limits for LBQS and Edinburgh quasars. Two conclusions can be drawn from this plot. First, the HDF quasars are extremely weak radio emitters. All twelve are below the traditional threshold for a radio-loud quasar,  $L_r = 10^{25} \text{ W Hz}^{-1}$ . In fact, all but one of the twelve are a factor of ten weaker than this limit, and 2 out of 12 are about a factor of 100 weaker than this limit. It is clear from Figure 4 that the great sensitivity of the HDF radio survey pushes the parameter space of radio luminosity for moderate redshift quasars. Also, there is no strong correlation between radio and optical luminosity for these samples.

We have identified six regions in Figure 3 for investigating the demographics of the radio-loud fraction. The sequence from 1 to 2 to 3 represents the cosmic evolution of the radio-loud fraction, in equal bins of one third of the look-back time, in the low luminosity range  $-25 < M_B < -22.5$ . The sequence from 1 to 4 to 6 represents the change in the radio-loud fraction with increasing optical luminosity by a factor of a thousand, in the redshift range  $0.02 < z < 3.64$ . We include the BQS sample in this comparison, noting that these quasars only contribute to the bin at low redshift and low luminosity (region 3) and the bin at high redshift and high luminosity (region 6).

Table 2 shows the statistics from these four samples combined, for three different definitions of the radio-loud fraction:  $\log L_r > 26$ ,  $\log L_r > 25$ , and  $\log L_r > 24 h_{50}^{-1} \text{ W Hz}^{-1}$ . All of the radio surveys have upper limits, but  $\log L_r > 26$  is above the limits in any of the surveys we are using. The criterion  $\log L_r > 25$  matches the most common definition in the literature, and it is immune from the nature of the radio non-detections for quasars less luminous than  $M_B = -26.5$  (see dashed box that defines upper limits in Figure 4). We note that all but one of the HDF quasars are radio-quiet at the level of  $\log L_r = 24$ , but the nature of the upper limits becomes important above a luminosity of  $M_B = -24$ . The footnotes in Table 2 give the number of quasars for which the designation radio-loud or radio-quiet is uncertain because the detection upper limit lies above the selected boundary in  $L_r$ . A lower limit on the radio-loud fraction can be estimated by assuming all of the uncertain quasars are radio-quiet — these values are also included in the footnotes to Table 2.

The data in the table show no trend for evolution in the radio-loud fraction of low luminosity quasars with cosmic time. A low radio-loud fraction of 0.05-0.10 is seen at all epochs (for  $L_r > 25$ ). In agreement with Goldschmidt et al. (1999), we see an increase in the radio-loud fraction with increasing optical luminosity. In the redshift interval  $0.84 < z < 3.64$ , the radio-loud fraction rises by a factor of 3-4 over a span of a factor of a thousand in optical luminosity. The low luminosity HDF quasars provide the strongest tether on this result, because 1/9 are radio-loud at any of the three radio thresholds.

#### 4. Conclusions

We have identified quasars selected from a multi-color survey with radio sources from a very deep catalog of a region centered on the northern Hubble Deep Field. The identification procedure accounts for the non-uniform radial distribution of radio sources over this region. Although limited by small number statistics, the result of the comparison is new information on the radio properties of low luminosity quasars at moderate redshift. We reach the following conclusions:

(1) Twelve optically selected quasars with  $B < 21$  and  $0.4 < z < 2.6$  are in the region within 20 arcmin of the HDF, which was covered in the deep radio survey of Richards (1999). Three of the quasars are identified with weak radio sources at greater than a 99.9% confidence level. The

remaining nine are below a  $3\sigma$  limit of 40 to 230  $\mu\text{Jy}$  at 1.4 GHz.

(2) The HDF quasars are extremely weak radio-emitters. All but one of the twelve have radio luminosities more than an order of magnitude below the traditional boundary between radio-loud and radio-quiet quasars,  $L_r = 10^{25} \text{ W Hz}^{-1}$ . Two of the twelve are about two orders of magnitude below that boundary, and are the lowest radio luminosity quasars ever measured at these redshifts.

(3) There is no strong evidence that radio and optical luminosity are correlated, a conclusion that is essentially independent of the nature of the radio non-detections. If we make a plausible assumption about the completeness of the optical quasar selection, no more than  $\sim 5\%$  of the radio source population above 230  $\mu\text{Jy}$  can be quasars at any optical brightness level.

(4) The fraction of quasars more radio luminous than  $10^{26} \text{ W Hz}^{-1}$  is 3-5% (or 5-10% above  $10^{25} \text{ W Hz}^{-1}$ ), independent of redshift over the range  $0.02 < z < 3.64$ . The fraction of quasars above  $10^{24} \text{ W Hz}^{-1}$  in radio luminosity shows slight evidence for an increase with increasing redshift. While the quasar space density evolves over two orders of magnitude, the probability of a quasar being a strong radio source is independent of epoch.

(5) The radio-loud fraction of quasars shows a marginally significant increase by a factor of three, going from low to high optical luminosity. This modest effect, combined with the lack of any strong correlation between radio and optical luminosity, means that the quasar radio luminosity function cannot be much flatter than the optical luminosity function.

We acknowledge useful discussions with Pippa Goldschmidt, Eric Hooper, Charles Liu, and Eric Richards. We are grateful to the referee for pointing out a significant error in the first version of this paper. CDI is grateful to the NSF for support under grant AST-9803072.

## REFERENCES

- Aller, M. F., Aller, H. D., and Hughes, P. A. 1992, *ApJ*, 399, 16
- Bischof, O., and Becker, R. H. 1997, *AJ*, 113, 2000
- Boyle, B. J., Shanks, T., and Peterson, B. A. 1988, in *Proceedings of a Workshop on Optical Surveys for Quasars*, eds. P. S. Osmer et al. San Francisco, ASP, p. 1.
- Cohen, J. G., Cowie, L. L., Hogg, D. W., Songaila, A., Blandford, R., Hu, E. M., and Shopbell, P. 1996 *ApJ*, 471, 5
- Condon, et al. 1998, *AJ*, 115, 1963
- Goldschmidt, P., Miller, L., La Franca, F., and Cristiani, S. 1992, *MNRAS*, 256, 65



- Goldschmidt, P., Kukula, M. J., Miller, L., and Dunlop, J. S. 1999, *ApJ*, 511, 612
- Grazian, A., Cristiani, S., D’Odorico, V., and Pizzella, A. 2000, submitted to the *Astrophysical Journal*, astro-ph/0002183
- Hall, P. B., Osmer, P. S., Green, R. F., Porter, A. C., and Warren, S. J. 1996, *ApJS*, 104, 185
- Hewett, P. C., and Foltz, C. B. 1994, *PASP*, 106, 113
- Hewett, P. C., Foltz, C. B., and Chaffee, F. H. 1995, *AJ*, 109, 1498
- Hooper, E. J., Impey, C. D., Foltz, C. B., and Hewett, P. C. 1995, *ApJ*, 445, 62
- Hooper, E. J., Impey, C. D., Foltz, C. B., and Hewett, P. C. 1996, *ApJ*, 473, 746
- Hogg, et al. 1998, *AJ*, 115, 1418
- Kellermann, K. I., Sramek, R., Schmidt, M., Green, R. F., and Shaffer, D. B. 1994, *AJ*, 108, 1163
- Kellermann, K. I., Sramek, R., Schmidt, M., Shaffer, D. B., and Green, R. 1989, *AJ*, 98, 1195
- Liu, C. T., Petry, C. E., Impey, C. D., and Foltz, C. B. 1999, *AJ*, 118, 1912
- Miller, P., Rawlings, S., and Saunders, R. 1990, *MNRAS*, 263, 425
- Miller, L., Peacock, J. A., and Mead, A. R. G. 1990, *MNRAS*, 244, 207
- Peacock, J. A., Miller, L., and Longair, M. S. 1986, *MNRAS*, 263, 425
- Richards, E. A., Kellermann, K. I., Fomalont, E. B., Windhorst, R. A., and Partridge, R. B. 1998, *AJ*, 116, 1039
- Richards, E. A. 1999, astro-ph/9908313
- Sandage, A. 1965, *ApJ*, 141, 1560
- Schmidt, M. 1963, *Nature*, 197, 1040
- Steidel, C. C., Giavalisco, M., Dickinson, M., and Adelberger, K.L. 1996, *AJ*, 112, 352
- Stocke, J., Morris, S. L., Weymann, R. J., and Foltz, C. B. 1992, *ApJ*, 396, 487
- White, R. L., Becker, R. H., Helfand, D. J., and Gregg, M. D. 1997, *ApJ*, 475, 479
- Williams, R. E., et al. 1996, *AJ*, 112, 1335
- Vanden Berk, D. E., Stoughton, C., Crofts, A. P. S., Tytler, D., and Kirkman, D. 2000, *AJ*, in press, astro-ph/0003203

Visnovsky, K. L., Impey, C. D., Foltz, C. B., Hewett, P. C., Weymann, R. J., and Morris, S. L. 1992, *ApJ*, 391, 560

Zitelli, V., Mignoli, M., Zamorani, G., Marano, B., and Boyle, B. J. 1992, *MNRAS*, 256, 349

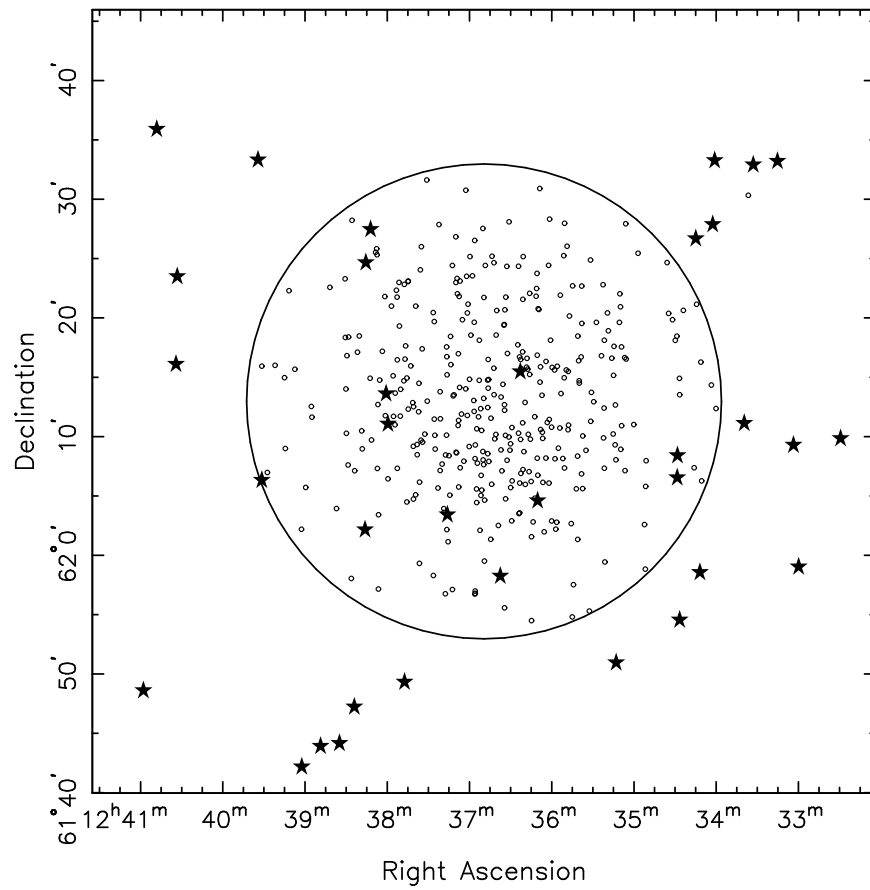


Fig. 1.— The one square degree field centered on the northern Hubble Deep Field (J2000). The 34 quasars are represented by filled stars (Liu et al. 1999; Vanden Berk et al. 2000). The 40' field of the radio survey (Richards 1999) is represented by the large circle, and the 372 radio sources are plotted as small open circles.

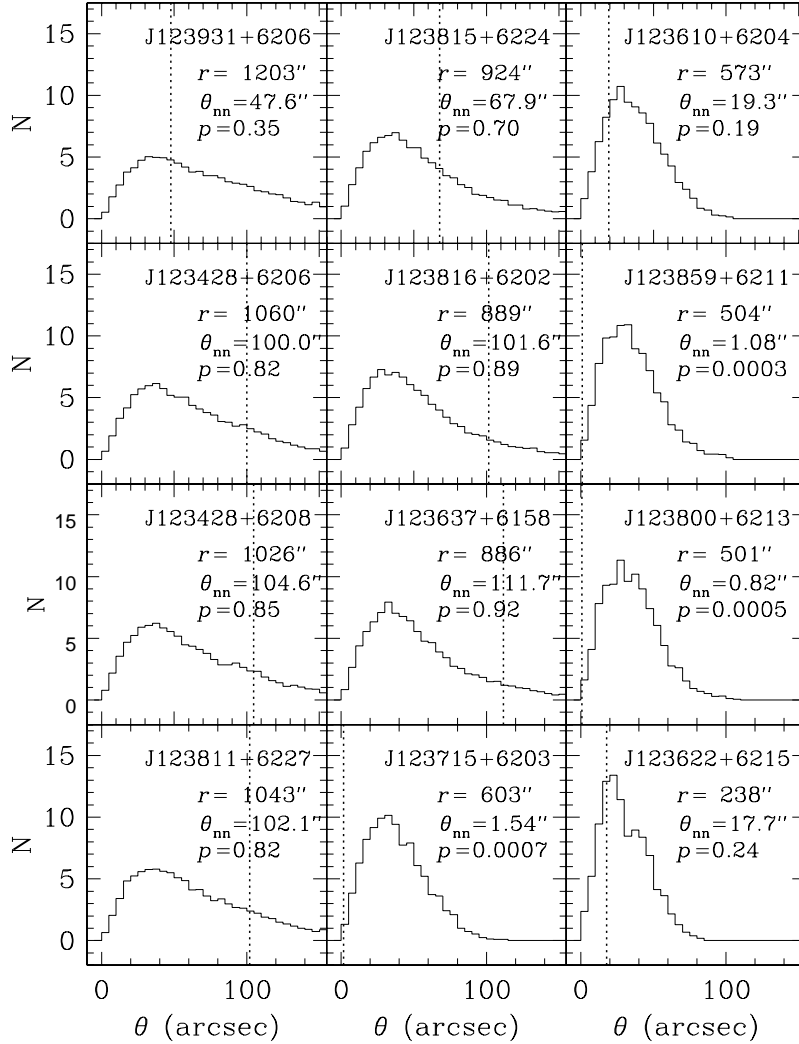


Fig. 2.— The results of a Monte Carlo simulation to test the significance of quasar identifications. The histograms show the distribution of distance to the nearest radio source for random placements of the quasar (measured at the appropriate radial distance from the HDF). Each panel is labelled with the name of the quasar, the radial distance of the quasar from the center of the field in arcseconds, the angular distance to the nearest radio source,  $\theta_{nn}$  (denoted graphically by the dotted vertical line), and the probability that the nearest neighbor is a chance counterpart (equal to the fraction of the histogram with  $\theta < \theta_{nn}$ ).

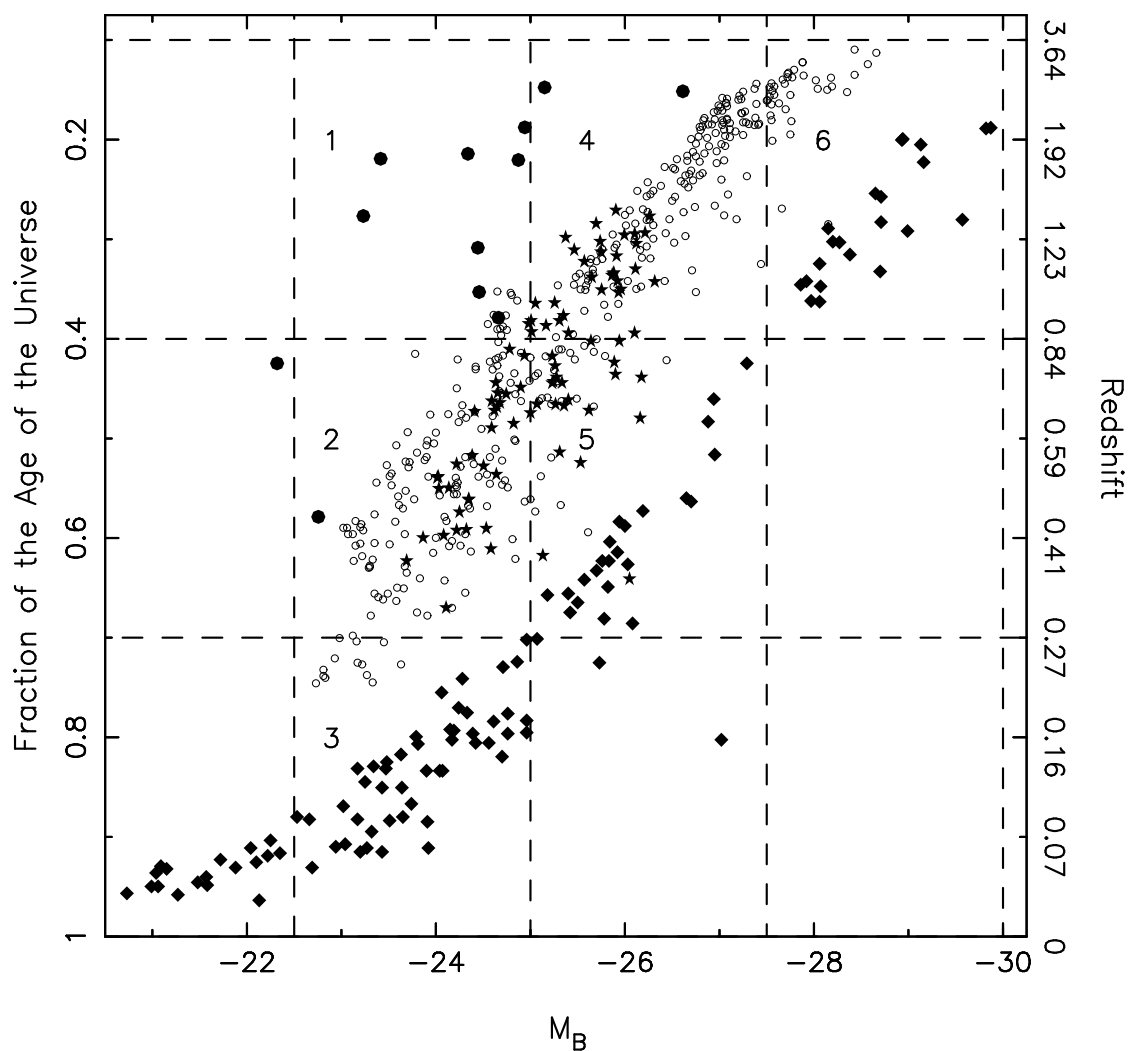


Fig. 3.— The coverage of the four samples in the optical luminosity–look-back time plane. The diamonds are the 114 BQS quasars, the small open circles are the 367 LBQS quasars, the stars are the 87 quasars from the Edinburgh survey, and the 12 HDF quasars are shown as large filled circles. The radio-loud fraction is investigated for the numbered regions defined by the dotted lines.

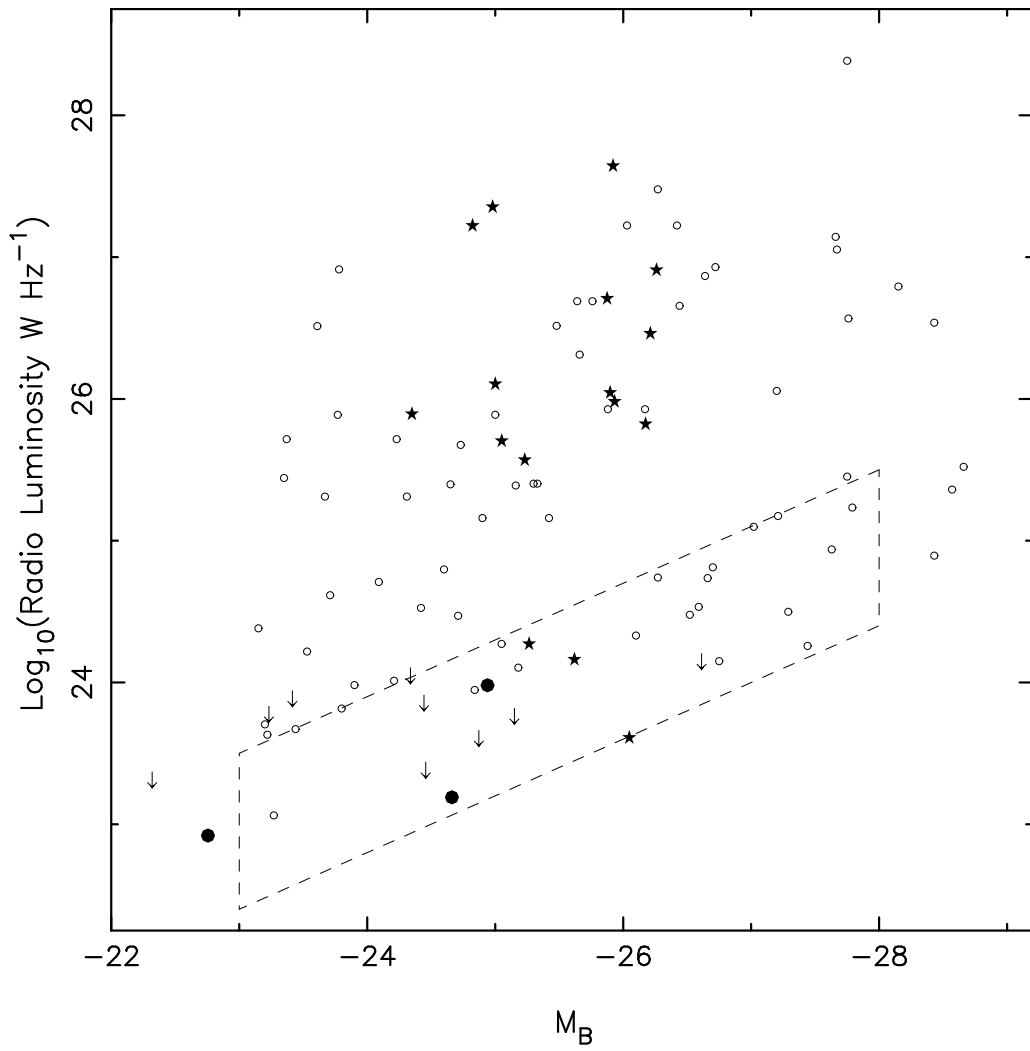


Fig. 4.— The optical luminosity – radio luminosity plane. The small open circles are the LBQS quasars, the stars are the Edinburgh survey quasars, and the HDF quasars are shown as large filled circles. The arrows are upper limits for HDF quasars. The region that encompasses the upper limits for the LBQS and Edinburgh surveys is shown as a dashed box.

Table 1. Quasars Within the HDF-N Radio Survey Area

Name	$\alpha$ (J2000)	$\delta$ (J2000)	$B$	$z$	Cross ID	$r^a$ (")	$\theta_{nn}^b$ (")	$S_{1.4}^c$ ( $\mu$ Jy)
J123428+6208	12 34 28.24	62 08 23.8	21.03	1.355*	...	1026	105	< 149
J123428+6206	12 34 28.41	62 06 32.1	20.47	1.793*	...	1060	100	< 162
J123610+6204	12 36 10.24	62 04 35.3	19.86	1.74	12	573	19.3	< 62
J123622+6215	12 36 22.89	62 15 27.4	20.50	2.58	13	238	17.7	< 42
J123637+6158	12 36 37.45	61 58 15.6	18.95	2.52	14	886	112	< 107
J123715+6203	12 37 15.96	62 03 24.5	20.18	2.05	15	603	1.55	109
J123800+6213	12 38 00.85	62 13 36.8	19.16	0.44	17	501	0.82	190
J123811+6227	12 38 11.99	62 27 27.5	20.76	0.77	18	1043	102	< 155
J123815+6224	12 38 15.46	62 24 40.7	21.33	1.75	19	924	67.9	< 117
J123816+6202	12 38 16.06	62 02 09.2	19.18	1.00	20	889	102	< 108
J123859+6211	12 37 59.51	62 11 03.4	18.77	0.910*	...	504	1.08	85
J123931+6206	12 39 31.44	62 06 20.1	19.54	1.19	25	1203	47.6	< 230

<sup>a</sup>The radial distance in arcseconds of each quasar from the center of the HDF.

<sup>b</sup>The angular distance in arcseconds from each quasar to the nearest radio source.

<sup>c</sup>The radio flux at 1.4 GHz (Richards 1999) of the source identified with each quasar. The upper bounds represent  $3\sigma$  limits, calculated using the gain curve of Richards (1999).

Note. — Quasar names, positions, and  $B$  magnitudes are from Vanden Berk et al. (2000). The redshift is quoted from Liu et al. (1999), except where marked with an asterisk to denote values taken from Vanden Berk et al. (2000). The sixth column is the cross-identification number from Table 1 of Liu et al. (1999).

Table 2. Radio-Loud Fraction

Region in Figure 3	Range	Fraction with $\log L_r > 26$	Fraction with $\log L_r > 25$	Fraction with $\log L_r > 24$
Redshift				
1	$3.64 < z < 0.84$	$0.048 \pm 0.049$	$0.095 \pm 0.070$	$0.300 \pm 0.197^a$
2	$0.84 < z < 0.27$	$0.025 \pm 0.012$	$0.080 \pm 0.023$	$0.143 \pm 0.034^b$
3	$0.27 < z < 0.0$	$0.033 \pm 0.024$	$0.049 \pm 0.029$	$0.066 \pm 0.034$
Optical Luminosity				
1	$-22.5 < M_b < -25.0$	$0.048 \pm 0.049$	$0.095 \pm 0.070$	$0.300 \pm 0.197^a$
4	$-25.0 < M_b < -27.5$	$0.077 \pm 0.021$	$0.118 \pm 0.028^c$	$0.674 \pm 0.162^d$
6	$-27.5 < M_b < -30.0$	$0.164 \pm 0.056$	$0.353 \pm 0.097^e$	$0.897 \pm 0.242^f$

<sup>a</sup>11/21 cases are uncertain,  $f_{\text{lim}} \gtrsim 0.143 \pm 0.088$ . <sup>b</sup>22/162 cases are uncertain,  $f_{\text{lim}} \gtrsim 0.123 \pm 0.029$ . <sup>c</sup>12/181 cases are uncertain,  $f_{\text{lim}} \gtrsim 0.110 \pm 0.026$ . <sup>d</sup>138/181 cases are uncertain,  $f_{\text{lim}} \gtrsim 0.160 \pm 0.032$ . <sup>e</sup>10/61 cases are uncertain,  $f_{\text{lim}} \gtrsim 0.295 \pm 0.079$ . <sup>f</sup>32/61 cases are uncertain,  $f_{\text{lim}} \gtrsim 0.426 \pm 0.100$ .

Note. — The footnoted values indicate that for the corresponding region, the designation of radio-loud or radio-quiet is uncertain for some number of quasars because the limiting radio flux is higher than the bound  $\log L_r > 24, 25$ , or 26. An approximate lower limit on the radio-loud fraction,  $f_{\text{lim}}$ , is computed assuming these quasars have  $L < L_r$  and are radio-quiet.